

Supplementary Materials for
Female reproductive life span is extended by targeted removal of fibrotic collagen from the mouse ovary

Takashi Umehara *et al.*

Corresponding author: Rebecca L. Robker, rebecca.robker@adelaide.edu.au

Sci. Adv. **8**, eabn4564 (2022)
DOI: 10.1126/sciadv.abn4564

This PDF file includes:

Figs. S1 to S12
Tables S1 and S2

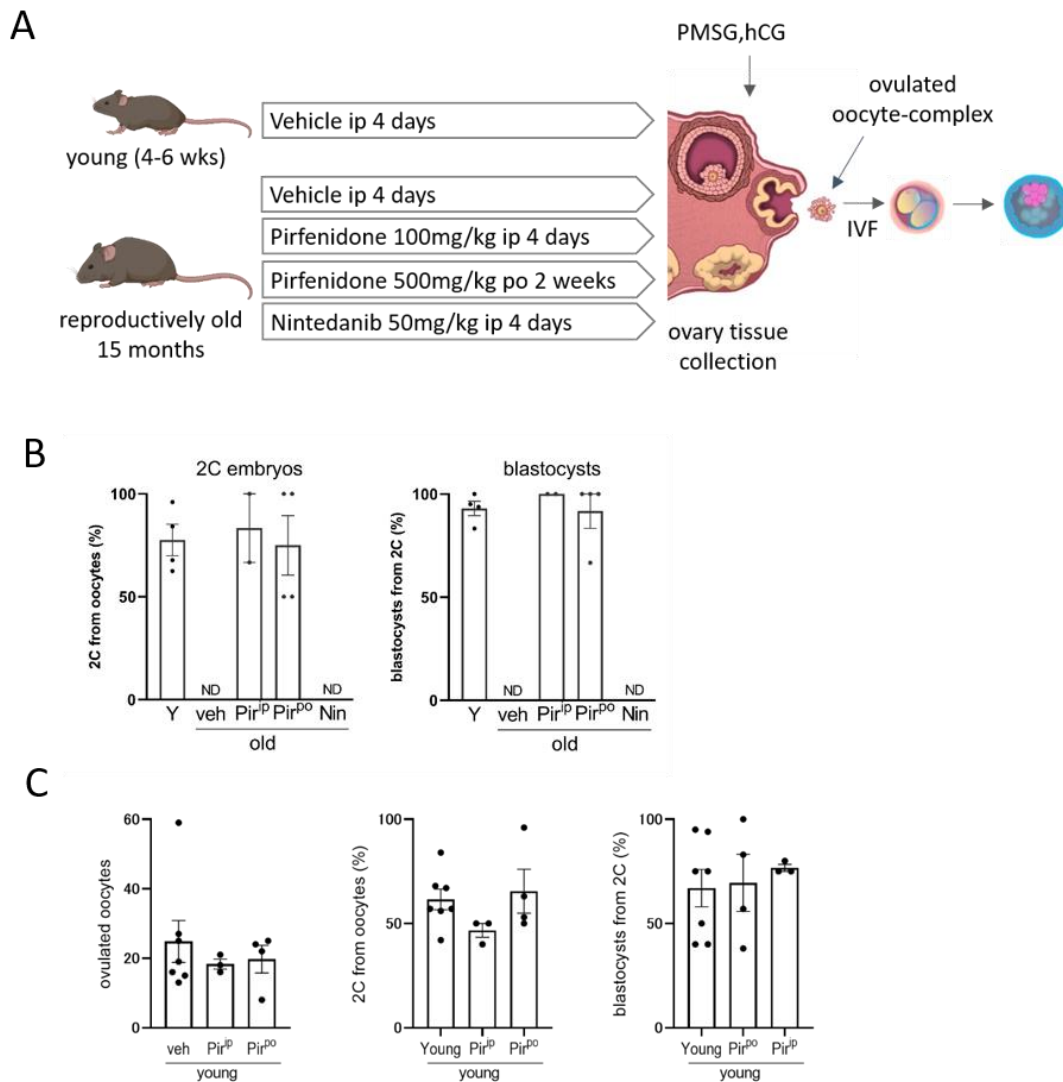


Fig. S1. Pirfenidone but not nintedanib facilitates ovulation in reproductively old mice.

Rationale for dosing: Pirfenidone has shown efficacy to reduce fibrosis in established mouse models using oral doses ranging from 100mg/kg body weight to 650mg/kg (70-73). Based on this information, we trialed pirfenidone at 100mg/kg but it was administered via daily intraperitoneal (ip) injection for 4 days in order to mimic our standard pre-ovulatory treatment protocol. In parallel, additional cohorts were given 500mg/kg in drinking water (po) for 2 weeks, a timeframe that would also encompass follicular development. In mouse models of fibrosis, nintedanib is typically administered by ip injection at doses ranging from 5mg/kg body weight to 50mg/kg (74, 75). **A**) Female mice that were 15 months old were treated with anti-fibrosis drugs pirfenidone (Pir), nintedanib (Nin) or vehicle (veh) as indicated and described in the Methods. Ovulated oocytes were collected at 15h post-hCG, counted and subjected to IVF. Ovulation and ovarian fibrosis data is shown in Figure 1. **B**) No ovulated oocytes (ND) were obtained from vehicle- or nintedanib-treated females. Oocytes from N=4 young females, n=2 old females given ip Pirfenidone (Pir^{ip}) and n=4 females given Pirfenidone orally (Pir^{po}) underwent IVF. Proportion of fertilized oocytes from each mouse that developed on-time to the 2 cell (2C) and blastocyst

stages is shown. All embryos appeared morphologically normal. **C)** Independent cohorts of young mice were treated with pirfenidone to verify that pirfenidone treatment is compatible with normal embryo development in young females. There were no differences in ovulation number (left), fertilization rate following IVF (middle), nor blastocyst development (right) in young mice treated with pirfenidone as in (A) compared to vehicle treated controls.

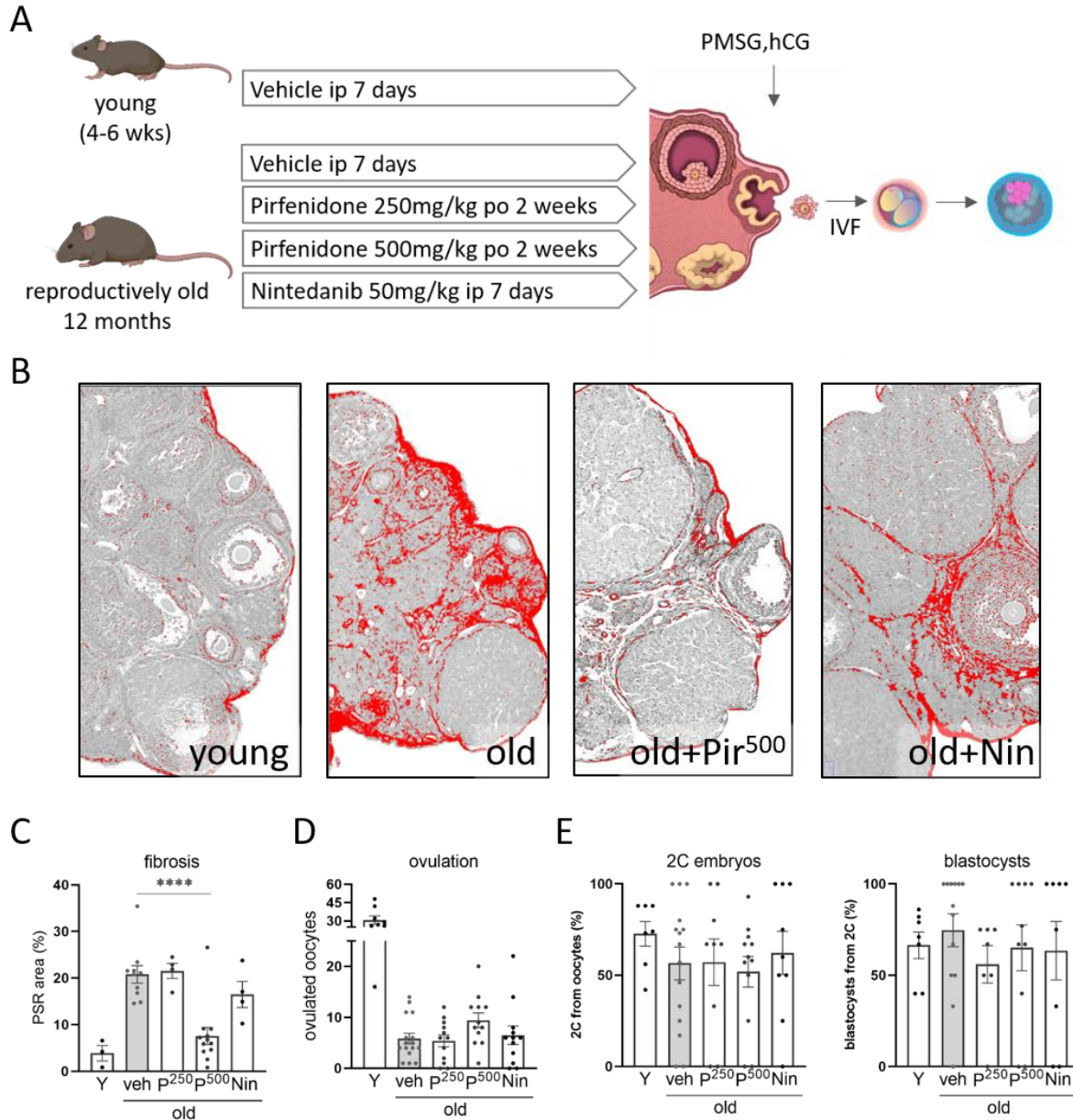


Fig. S2. Ovarian fibrosis occurs in 12 month old mice and is reversed by pirfenidone. Rationale for dosing: Pirfenidone was administered at 500mg/kg for 2 weeks as this dose improved ovulation in initial experiments (Fig 1); and at 250mg/kg in order to determine whether a lower dose would also show efficacy. Nintedanib was trialed again at 50mg/kg daily via intraperitoneal (ip) injection but this time for 7 days to determine if longer administration would show efficacy. **A)** Female mice that were 12 months old were treated with anti-fibrosis drugs pirfenidone (Pir) or nintedanib (Nin) as indicated and described in the Methods. Ovulated oocytes were collected at 15h post-hCG, counted and subjected to IVF. **B)** Representative ovarian sections stained with Picrosirius Red (PSR) and scanned for imaging. **C)** Quantification of PSR stain in the ovarian stroma. **D)** Number of ovulated oocytes from each mouse. **E)** Proportion of fertilized oocytes from each mouse that developed on-time to the 2 cell (2C) and blastocyst stages. All embryos appeared morphologically normal.

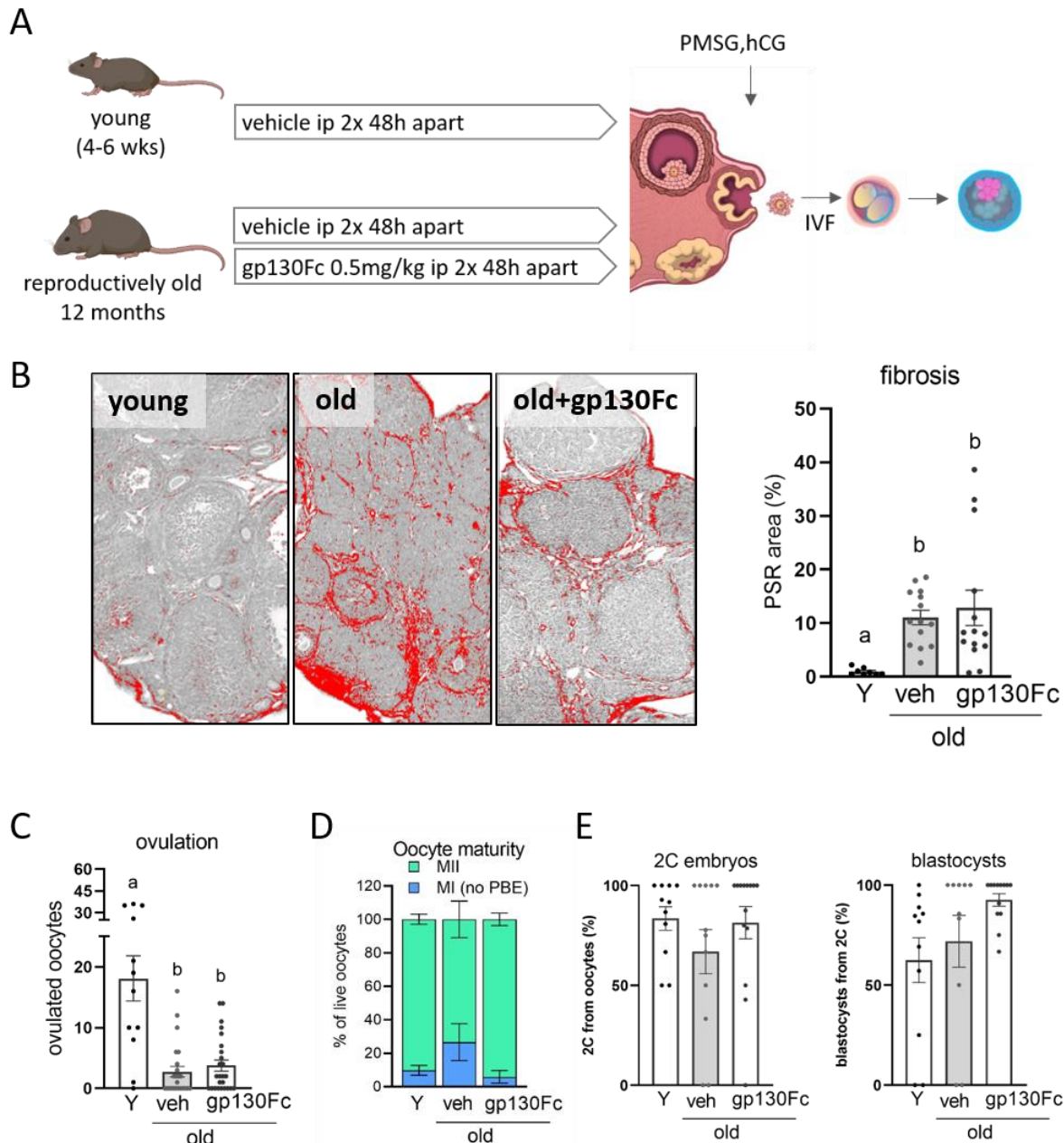


Fig. S3. Olamkipept (sgp130Fc) does not influence ovarian fibrosis or ovulation in reproductively aged mice. **A)** Female mice that were 12 months old were treated with olamkipept (sgp130Fc) or vehicle (veh) as indicated and described in the Methods, based on identical dose and timing as in (19). Ovulated oocytes were collected at 15h post-hCG, counted and subjected to IVF. **B)** Representative ovarian sections stained with Picrosirius Red (PSR) and scanned for imaging. Right panel: Quantification of PSR stain in the ovarian stroma. ANOVA (a vs b) $p < 0.01$. **C)** Number of ovulated oocytes from each mouse. $N=12$ young; $n=24$ old; $n=25$ old+sgp130Fc. ANOVA (a vs b) $p < 0.0001$. **D,E)** Oocytes were obtained from $n=11$ young, $n=12$ old and $n=14$ old+sgp130Fc mice. **D)** Assessment of oocyte maturation prior to IVF in each mouse. Normal maturation to MII was determined by visible polar body extrusion (PBE). **E)** Proportion of fertilized oocytes from each mouse that developed on-time to the 2 cell (2C) and blastocyst stages. All embryos appeared morphologically normal.

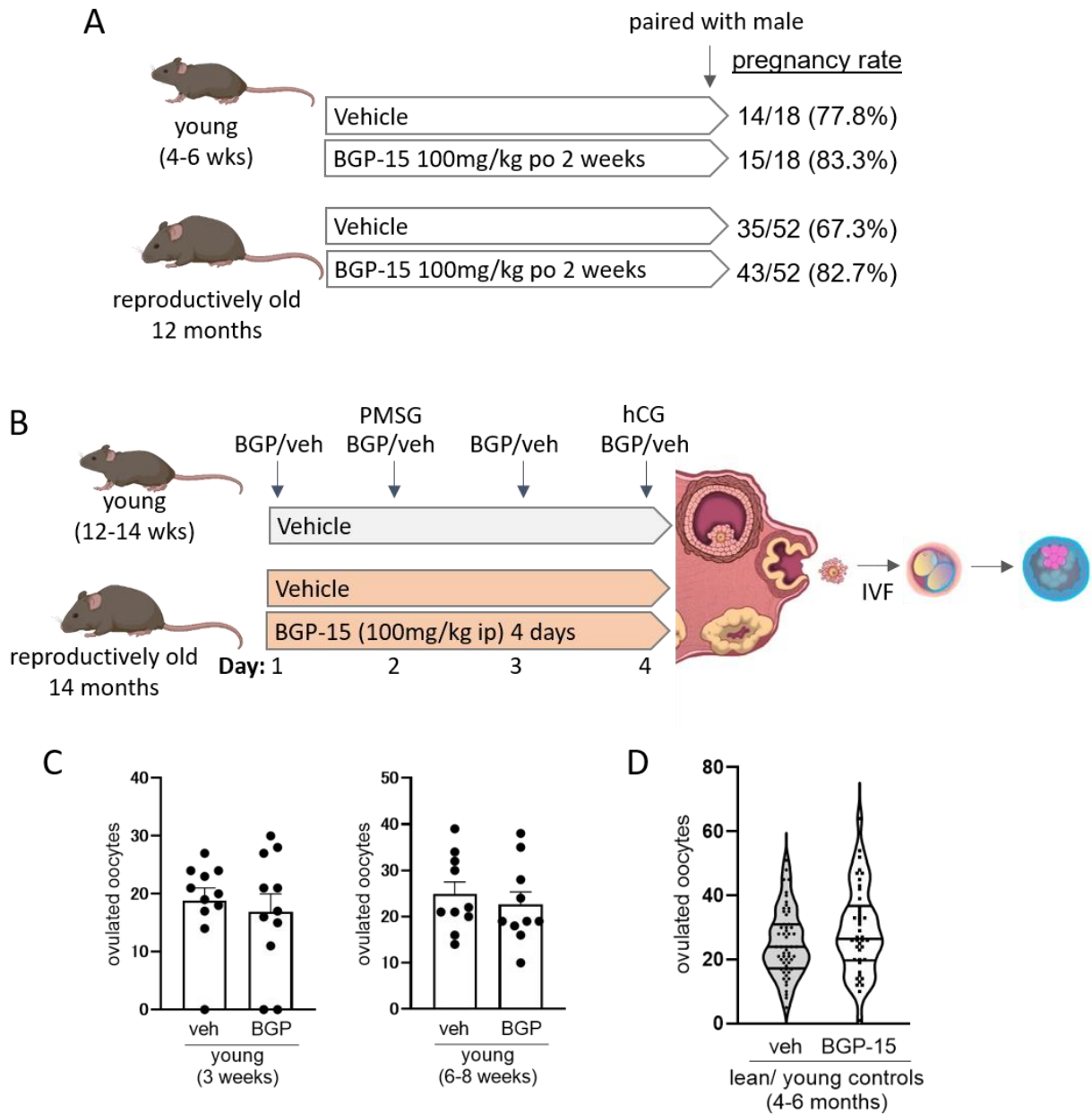


Fig. S4. Experimental design for administering BGP-15 to reproductively aged mice and assessing fertility.

Rationale for dosing: Our standard protocol is to administer BGP-15 at 100mg/kg body weight by daily intraperitoneal (ip) injection for 4 days as in (35), an effective dose also adopted by others (28). BGP-15 is also administered orally, in human clinical trials, and in mouse models where it is typically provided in drinking water or by gavage for between 5 days and 4 weeks (27, 29, 30, 76). For oral administration we continued with the 100mg/kg dose. **A)** Female mice that were young or reproductively old (12 months) were treated with or without BGP-15 (100mg/kg body weight) in drinking water for 2 weeks as indicated and described in the Methods. Females were then paired with males and pregnancy was determined by an increase in body weight ($\geq 3g$) one week later. Numbers of females per group and percent that became pregnant are shown. **B)** After their pups

were weaned, female mice (now 14 months old) were given BGP-15 (100mg/kg) via daily ip injection for 4 days concurrent with gonadotropins as indicated and per our previous study (35). Ovulated oocytes were collected at 15h post-hCG, counted and subjected to IVF followed by monitoring to the blastocyst stage. Ovarian fibrosis, ovulation and embryo development from a subset of these mice is shown in Figure 2. **C)** To examine the effects of BGP-15 on ovulation capacity in young females, independent cohorts of C57 mice at 3 weeks of age (left panel) or 6-8 weeks of age (right panel) were treated with BGP-15 (100mg/kg) via daily ip injection for 4 days concurrent with gonadotropins (or saline vehicle). Analysis by unpaired t-test showed no difference between treatment groups. **D)** Cohorts of lean young female mice (4-6 months of age) were treated with BGP-15 (100mg/kg) via daily ip injection for 4 days concurrent with gonadotropins, in parallel to vehicle-treated controls (also shown in Fig. 4F). n=56 veh-treated and n=42 BGP-15 treated females; p=0.122 by unpaired t-test.

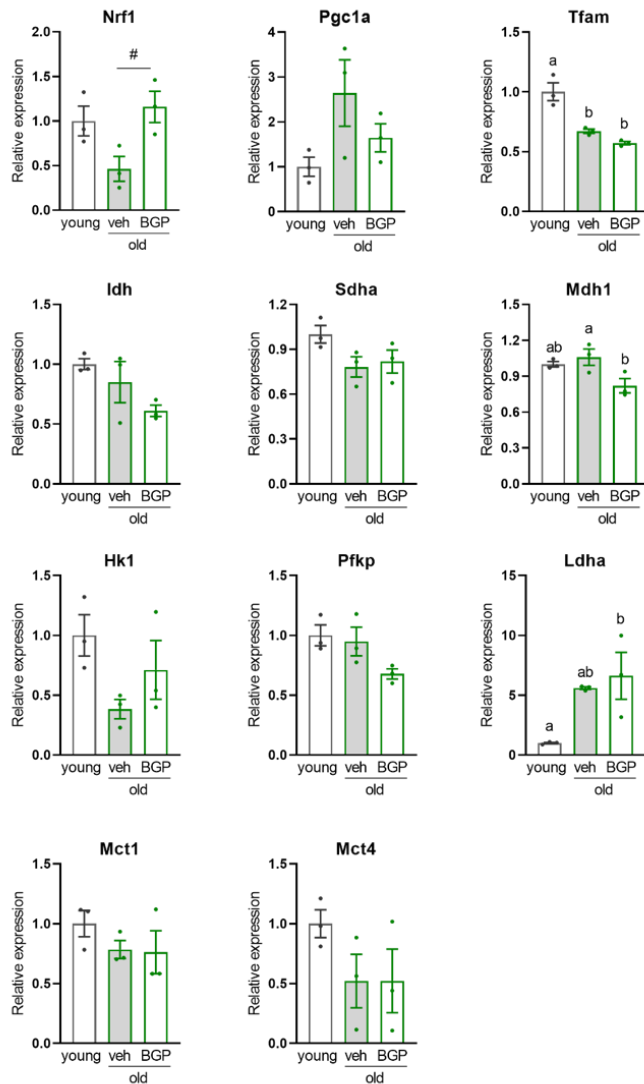


Fig. S5. Mitochondria and metabolism-related genes in the ovarian stromal cells of reproductively aged mice are not significantly altered by BGP-15 treatment.

Gene expression in ovarian stromal cells of mice that were young or old and treated with BGP-15 as in Supp Fig 4B and Figure 2. Gene expression was normalized to reference gene *L19* and presented relative to controls. Values represent mean \pm SEM of 3 replicate pools of stromal cells from multiple mice. Different letters indicate significant differences ($p < 0.05$) by One-way ANOVA. # $p = 0.051$.

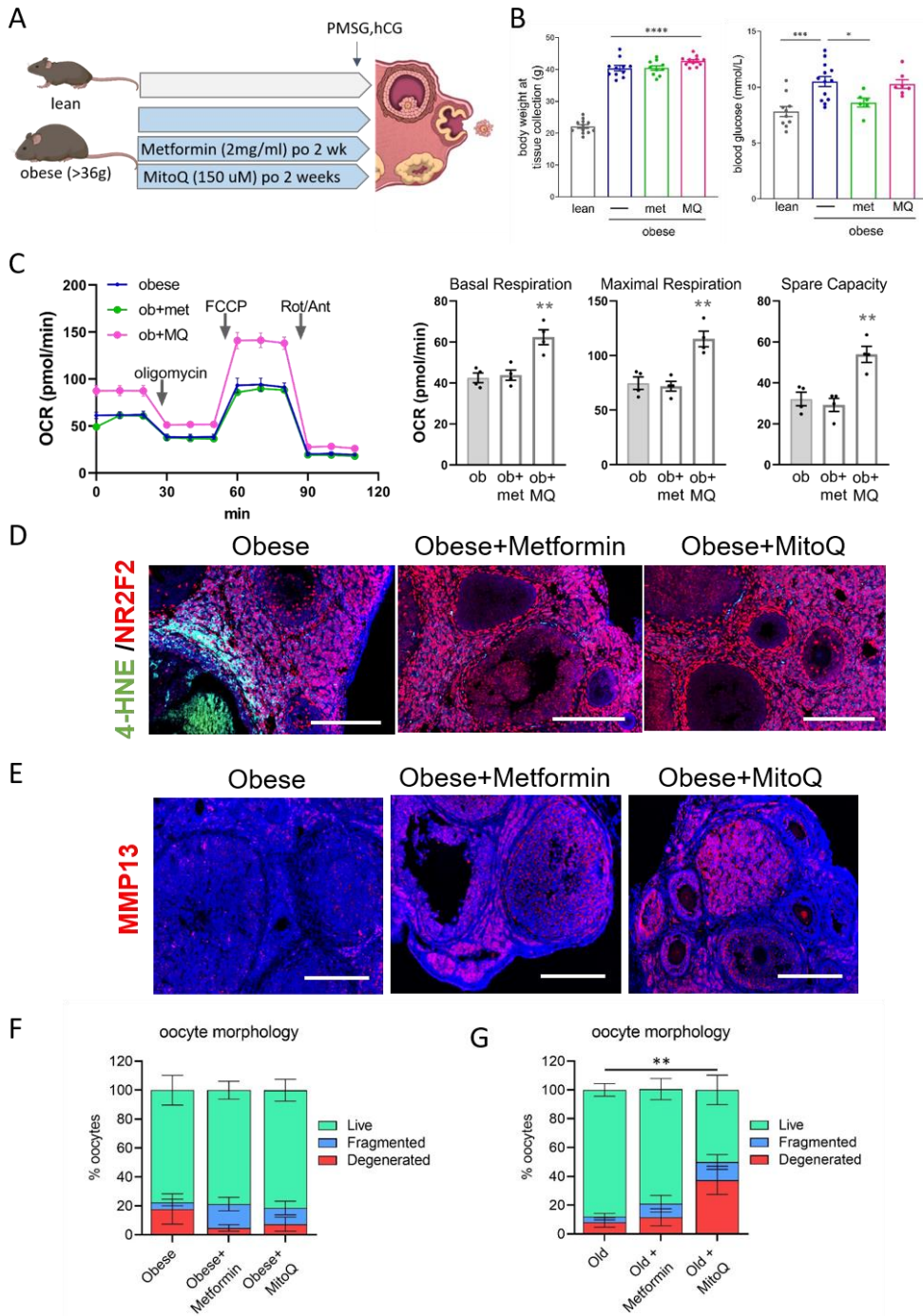


Fig. S6. Metformin and MitoQ exert distinct effects on metabolism, ovarian fibrosis markers and oocyte quality in obese and reproductively old mice.

Rationale for dosing: A review of published studies found that in mouse models of metabolic disease metformin is commonly used and shows efficacy at 2mg/ml in drinking water. For MitoQ, a dose of 250 μ M in drinking water was initially trialed based on the anti-oxidant effects observed by others (77), however the mice exhibited taste aversion (ie reduced water consumption). Thus the dose was lowered 150 μ M MitoQ, no taste aversion was observed and this dosing protocol was used for all experiments.

A) Obese (ob) mice were untreated or given metformin (met) or MitoQ (MQ) in drinking water for 2 weeks as indicated and described in the Methods, followed by collection of ovaries and oviducts at 15h post-hCG. **B)** Body weight and non-fasted blood glucose levels at tissue collection. Statistical analysis by One-way ANOVA shows all obese females had higher body weight than controls ($p < 0.0001$) that was not influenced by metformin or MitoQ treatment; and that elevated blood glucose in obese mice ($p < 0.001$) was normalized by metformin ($p < 0.05$). Ovarian fibrosis and ovulation in these mice is shown in Figure 5. **C)** Stromal cells isolated from ovaries underwent a Mito Stress Test using Seahorse XF Analyzer and the optimized conditions as in described in Methods. Values represent mean \pm SEM of 4 to 6 wells containing cells pooled from 2 mice. Right panels: Basal respiration, maximal respiration and spare capacity determined from Oxygen Consumption Rate (OCR) **D)** Representative examples of oxidative stress marker 4-HNE in ovarian sections using anti-4-HNE antibody (green) and anti-NR2F2 stromal cell marker (red). **E)** Representative examples of immuno-localization of MMP13 in ovaries using anti-MMP13 antibody (red) and DAPI nuclear counterstain. Scale bar: 200 μ m. **F)** Morphology assessment of ovulated oocytes of obese mice and those treated with either metformin or MitoQ. N=11 females per group. **G)** Reproductively old mice (Aged) were untreated or treated with either metformin or MitoQ, exactly as for obese mice in A. (Ovarian fibrosis and ovulation in these old mice is shown in Figure 5.) Morphology assessment of ovulated oocytes: n=21 (old females), n=19 (old+met), n=17 (old+MQ). **F,G)** Proportion of degenerated oocytes was analyzed by ANOVA, ** $p < 0.01$.

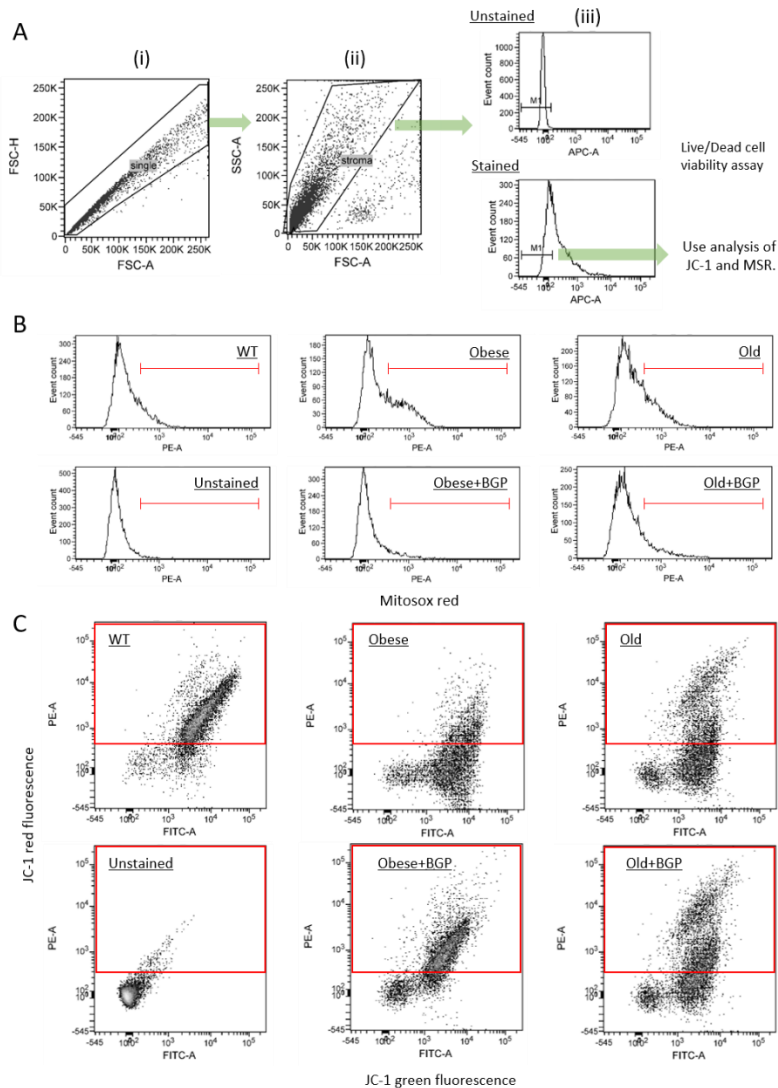


Fig. S7. Gating strategy and representative raw data of flow cytometry analysis of mouse ovarian stromal cells.

A) Gating strategy of Mitosox red (MSR) and JC-1 analysis using FACSAnalyzer. (i) Single cells were selected using tight FSC-H/FSC-A discrimination gate. (ii) Stromal cells were selected using a SSC-A/FSC-A discrimination gate. (iii) Using Live/Dead cell viability dye, live cells (intensity less than 1×10^2) were selected, and used for analysis of MSR and JC-1. **(B)** Histograms of MSR staining. Red line indicates the range of positive cells used in Figure 6D. **(C)** Analysis of JC-1 staining. FITC-A indicates JC-1 green fluorescence and PE-A indicates JC-1 red fluorescence. Red boxes indicate the area of positive cells used in Figure 6C. WT: lean young controls.

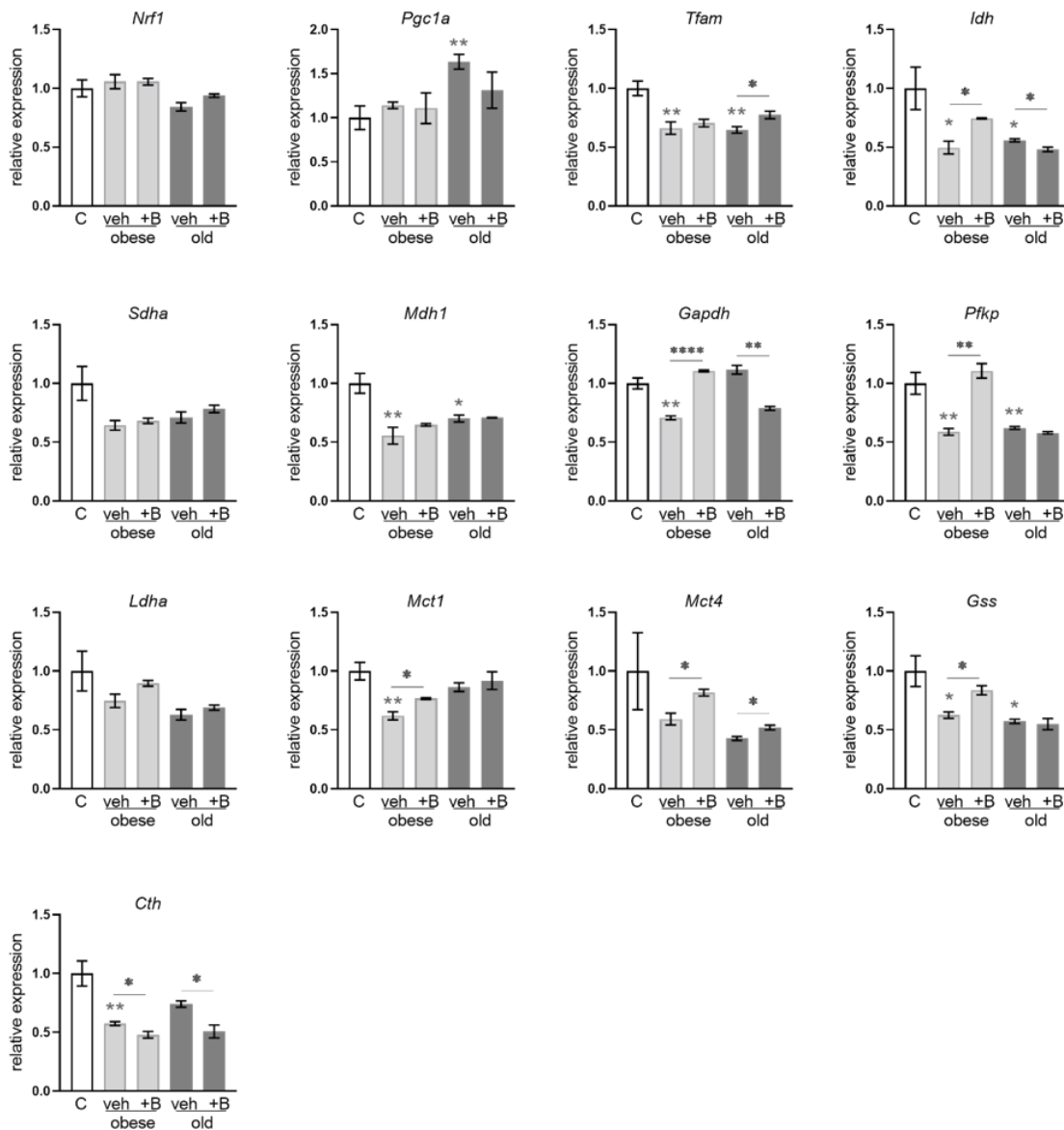


Fig. S8. Mitochondria and metabolism-related genes in ovarian stromal cells are only subtly dysregulated by obesity, aging and BGP-15 treatment.

Gene expression in ovarian stromal cells of mice that were obese or old and treated with BGP-15 (+B), or not (veh), as well as young lean controls (C); as depicted in Figure 4D. Gene expression was normalized to reference gene *L19* and presented relative to controls. Values represent mean \pm SEM of $n=3$ samples of mRNA pooled from multiple mice. * $P<0.05$; ** $P<0.01$; **** $P<0.0001$ by One-way ANOVA compared to controls or by two-tailed t-test compared to veh-treated mice, as indicated.

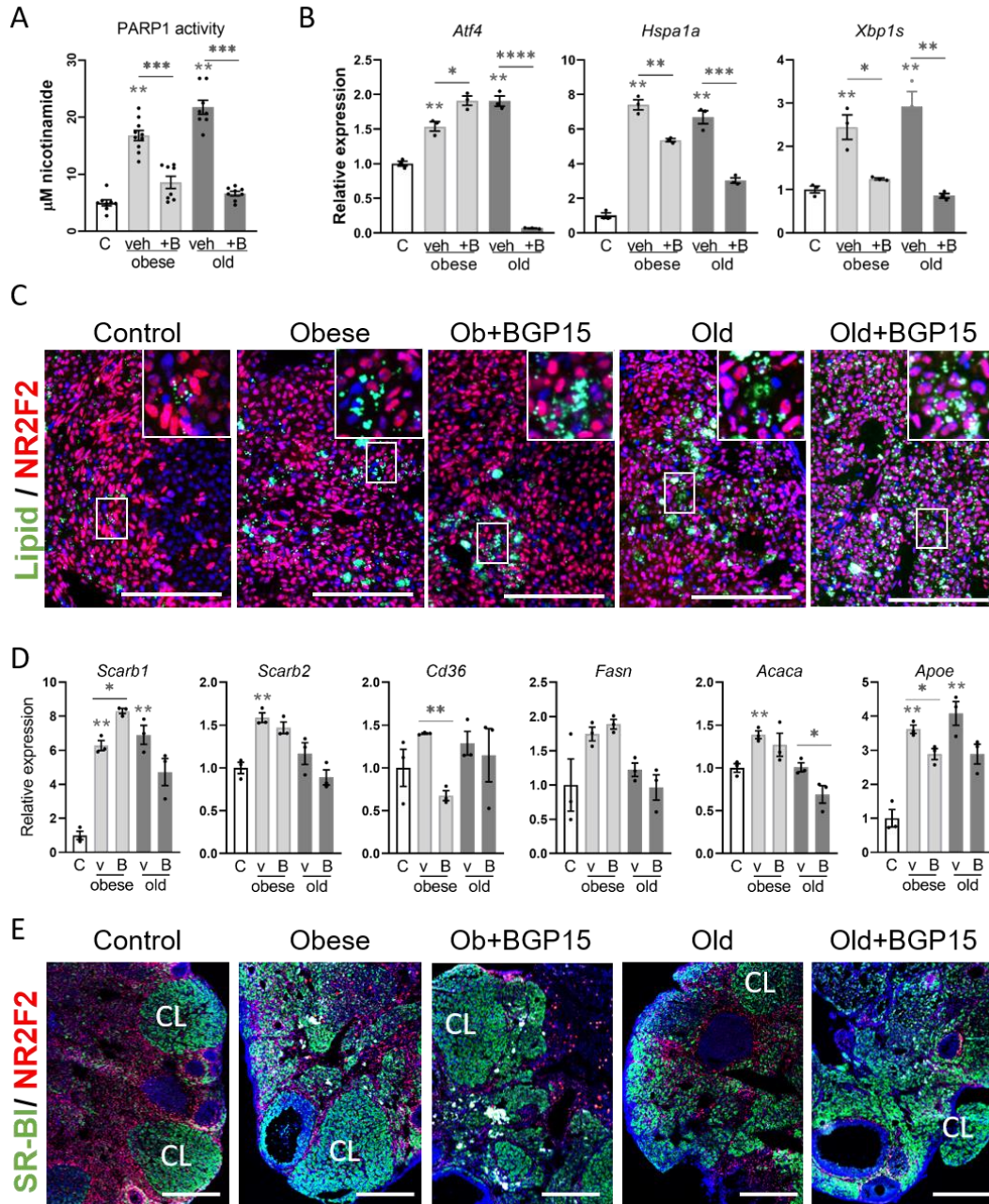


Fig. S9. DNA damage and ER stress, but not lipogenesis, is normalized by BGP-15 treatment of obese and reproductively old mice.

A) PARP1 activity was measured by enzyme activity assay and normalized to total protein in ovarian stromal cells of control (C), obese and old mice treated with BGP-15 (B) or vehicle (veh), as depicted in Figure 4D. **B)** Expression of *Atf4*, *Hspa1a*, and *Xbp1s*, markers of endoplasmic reticulum stress, in ovarian stromal cells of control, obese and old mice treated with BGP-15 or vehicle. Gene expression was normalized to reference gene *L19* and presented relative to controls. Values represent mean \pm SEM of $n=3$ samples of mRNA pooled from multiple mice. **C)** Localization of lipid droplets in the ovary of control, obese and old mice treated with BGP-15 or vehicle. Sections were stained using Nile red neutral lipid stain (which

fluoresces green) and anti-NR2F2 antibody (red). Scale bar:100 μ m. Boxed area is shown at higher magnification in inset. **D**) Expression of genes involved in intake of fatty acid and cholesterol (*Scarb1*, *Scarb2*, *Cd36*), fatty acid biogenesis (*Fasn*, *Acaca*), and transport of fatty acid (*ApoE*) in ovarian stromal cells of control (C), obese and old mice treated with BGP-15 (B) or vehicle (v). Expression levels were normalized to that of *L19*, and presented relative to controls. Values represent mean \pm SEM of 3 replicate pools of stromal cells from multiple mice. **E**) Localization of scavenger receptor B1 (SR-BI) in the ovary. Sections were stained using anti-SR-BI antibody (green) and anti-NR2F2 antibody (red). Scale bar:100 μ m. CL: corpus luteum. * $P < 0.05$; ** $P < 0.01$; *** $P < 0.001$; **** $P < 0.0001$ by one-way ANOVA compared to controls or by two-tailed t-test between BGP-15-treated and vehicle-treated mice as indicated.

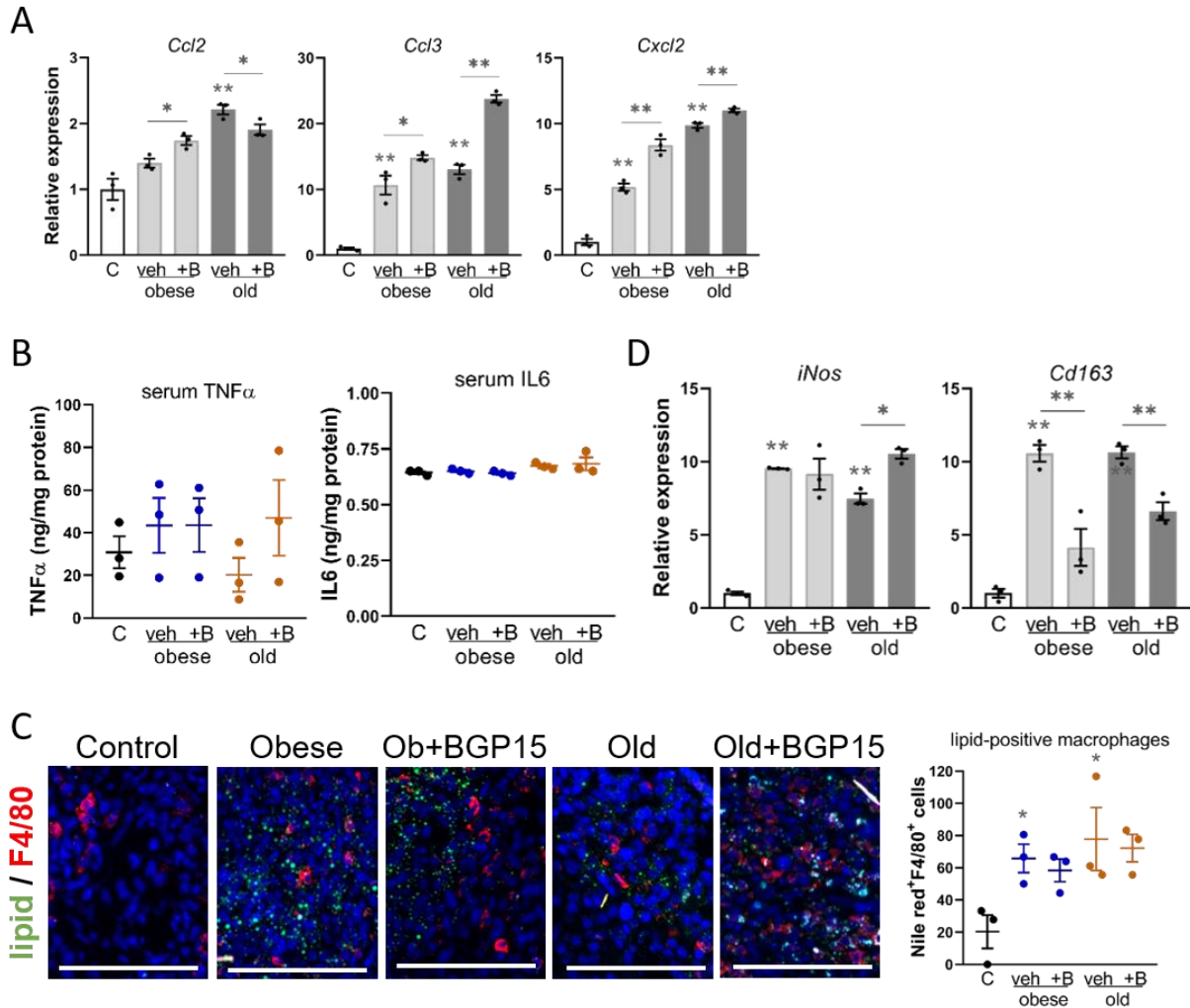
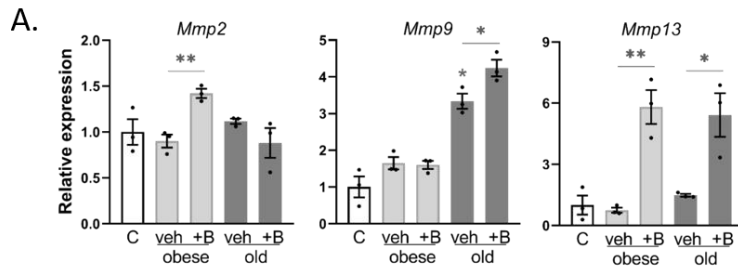


Fig. S10. Elevated CD163 gene expression, but not other inflammatory markers, is normalized by BGP-15 treatment of obese and reproductively old mice.

A) Gene expression of chemokines (*Ccl2*, *Ccl3*, *Cxcl2*) in ovarian stromal cells of control (C), obese and old mice treated with BGP15 (+B) or vehicle (veh), as depicted in Figure 4D. Expression was normalized to that of *L19*, and presented relative to controls. Values represent mean \pm SEM of n=3 samples of mRNA each pooled from multiple mice. **B**) Concentration of TNF α and IL6 in serum by ELISA. Values represent mean \pm SEM of n=3-4 replicate samples of material pooled from multiple mice. **C**) Localization of lipid droplets in macrophages by immunohistochemistry using anti-F4/80 antibody (red) and Nile red neutral lipid stain (fluoresces green). Right panel: Numbers of F4/80-Nile red double positive cells in the ovarian stroma. **D**) Expression of *iNos* and *Cd163* in ovarian stromal cells, as in panel A. *P<0.05; **P<0.01 by one way ANOVA compared with controls or by two-tailed t-test compared to vehicle treated mice as indicated.



B.

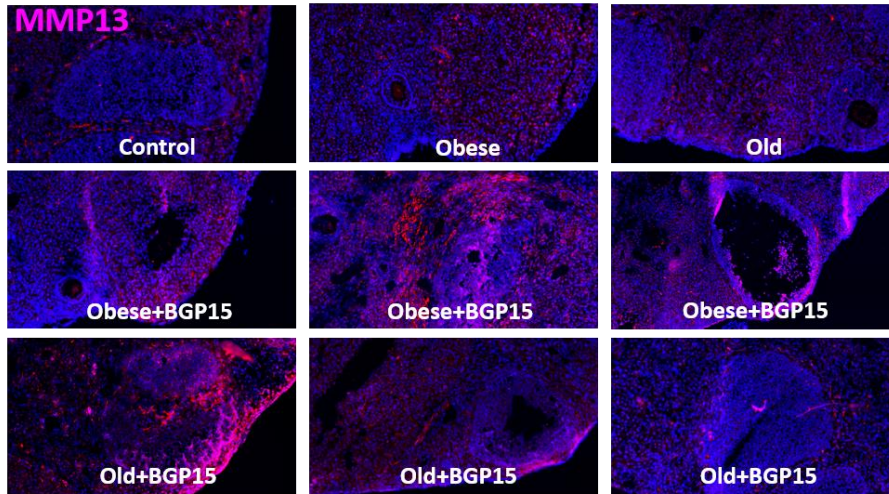


Fig. S11. Matrix metalloprotease MMP13 is dramatically upregulated in response to BGP-15 in ovarian stroma of both obese and reproductively old mice.

A) Gene expression of matrix metalloproteases (*Mmp2*, *Mmp9*, *Mmp13*) in ovarian stromal cells of control (C), obese and old mice treated with BGP15 (+B) or vehicle (veh), as depicted in Figure 4D. Expression was normalized to that of reference gene *L19*, and presented relative to controls. Values represent mean \pm SEM of n=3 replicate pools of stromal cells. **B)** Additional examples of localization of MMP13 in ovaries of mice that are obese or old, with or without BGP15 treatment and controls, as per Figure 8D. *P<0.05; **P<0.01 by one way ANOVA compared with controls or by two-tailed t-test compared to vehicle treated mice as indicated.

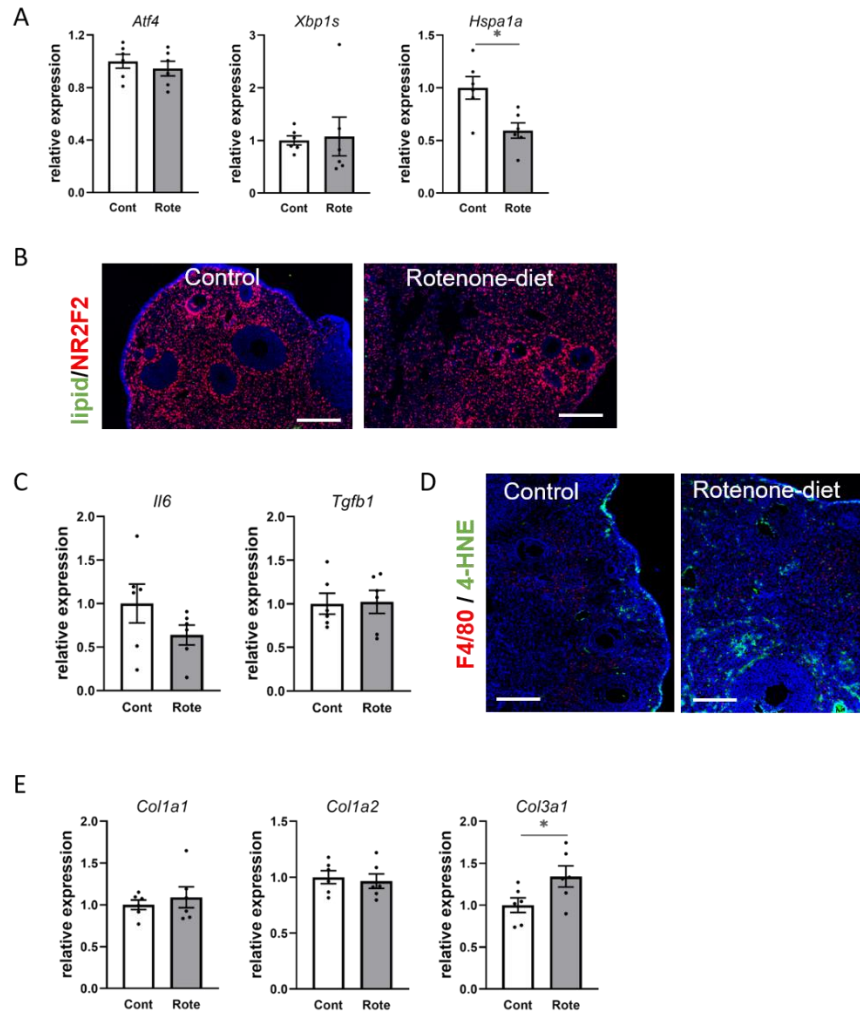


Fig. S12. Only a subset of fibrosis markers are induced in ovarian sections or stromal cells of mice exposed to a Complex I inhibitor (rotenone).

Young mice were fed a rotenone-containing diet (150ppm) or matched control diet for 3 weeks, as described in the Methods and in Figure 9. **A**) Expression of ER stress genes (*Atf4*, *Xbp1s*, *Hspa1a*) in ovarian stromal cells of mice fed rotenone-diet (Rote) or matched control diet (Cont) for 3 weeks. Expression was normalized to that of reference gene *L19*, and presented relative to controls. Values represent mean \pm SEM of stromal cells from individual mice. **B**) Example of Nile red neutral lipid stain (fluoresces green) co-localized with stromal marker NR2F2 (red) in ovarian sections and counterstained with DAPI nuclear dye. Lipid accumulation was not detected, likely due to the relatively young age of the mice. **C**) Expression of *Il6* (inflammatory cytokine) and *Tgfb1* (anti-inflammatory cytokine) in ovarian stromal cells as in panel A. Expression of *Tnfa*, *Il4*, *Il13* and *Infg* was undetectable in cells from both control-diet and rotenone-fed mice, likely due to their relatively young age. **D**) Example of macrophage localization by immunohistochemistry using anti-F4/80 antibody (red), and co-labeling with anti-4-HNE (green). F4/80 positive cells were counted and are shown in Figure 9D. **E**) Expression of collagen genes (*Col1a1*, *Col1a2*, *Col3a1*) in ovarian stromal cells as in panel A. * $p < 0.05$ by two-tailed t-test.

Table S1. Antibodies for immunohistochemistry (IF) and Western blot (WB)

Antigen	Cat No.	Company	Species	IF	WB
Collagen I	NB600-408	Novus	Mouse	1:100	
NR2F2	ab211777	abcam	Rabbit	1:500	
4-HNE	ab48506	abcam	Mouse	1:100	
iNOS	ab49999	abcam	Mouse	1:100	
CD163	ab182422	abcam	Rabbit	1:100	
F4/80	ab100790	abcam	Rabbit	1:100	
MMP13	ab39012	abcam	Rabbit	1:100	1:500
SR-BI	NB400-131	Novus	Rabbit	1:100	
DNA/RNA Damage Antibody (15A3)	NB110-96878	Novus	Mouse	1:50	
Histone 3	9715	Cell signaling	Mouse		1:1000
F4/80	sc-377009	Santa cruz	Mouse	1:100	
MMP13	MA5-14238	Invitrogen	Mouse	1:100	
Goat anti-Mouse IgG Alexa Fluor 594	A11032	Invitrogen		1:2000	
Goat anti-Rabbit IgG Alexa Fluor 594	A11037	Invitrogen		1:2000	
Goat anti-Rabbit IgG Alexa Fluor 488	A11034	Invitrogen		1:2000	
Goat anti-Mouse IgG Alexa Fluor 488	A11001	Invitrogen		1:2000	

Table S2. Taq-man Assay Primer Sets (ThermoFisher)

<i>Gene Name</i>	Taq-man Assay
<i>Acaca</i>	Mm01304257_m1
<i>Amh</i>	Mm00431795_g1
<i>Apoe</i>	Mm01307193_g1
<i>Atf4</i>	Mm00515325_g1
<i>Bmp15</i>	Mm00437797_m1
<i>Ccl2</i>	Mm00441242_m1
<i>Ccl3</i>	Mm00441258_m1
<i>Cd163</i>	Mm00474091_m1
<i>Cd36</i>	Mm00432403_m1
<i>Colla1</i>	Mm00801666_g1
<i>Colla2</i>	Mm 00483937
<i>Col3a1</i>	Mm00802300_m1
<i>Cxcl2</i>	Mm00436450_m1
<i>Fasn</i>	Mm00662319_m1
<i>Fshr</i>	Mm00442819_m1
<i>Hspa1a</i>	Mm01159846_s1
<i>Il13</i>	Mm00434204_m1
<i>Il4</i>	Mm00445259_m1
<i>Il6</i>	Mm00446190_m1
<i>Infg</i>	Mm00801778_m1
<i>iNos</i>	Mm00440502_m1
<i>Mmp2</i>	Mm00439498_m1
<i>Mmp13</i>	Mm00439491_m1
<i>Mmp9</i>	Mm00442991_m1
<i>Rpl19</i>	Mm02601633_g1
<i>Scarb1</i>	Mm00450234_m1
<i>Scarb2</i>	Mm00446977_m1
<i>Tgfb1</i>	Mm01178820_m1
<i>Tnf</i>	Mm00443258_m1
<i>Xbp1</i>	Mm00457357_m1